

NUMERICAL CODE FOR FITTING RADIAL EMISSION PROFILE OF A SHELL SUPERNOVA REMNANT. APPLICATION

S. Opsenica and B. Arbutina

*Department of Astronomy, Faculty of Mathematics, University of Belgrade
Studentski trg 16, 11000 Belgrade, Serbia*

E-mail: *slobodan@math.rs, arbo@math.rs*

(Received: October 21, 2011; Accepted: October 31, 2011)

SUMMARY: We present IDL (Interactive Data Language) codes for fitting a theoretical emission profile of a shell supernova remnant (SNR) to the mean profile of an SNR obtained from radio observations. Two considered theoretical models are: 1) a shell with constant emissivity and 2) a synchrotron shell with radially aligned magnetic field. The codes were applied to several observed supernova remnants. Good results are obtained in five considered cases, which justify the use of our code for remnants that are bright (so that observational errors are not large) and spherically symmetric enough.

Key words. ISM: supernova remnants – radio continuum: ISM – methods: numerical – ISM: individual objects: G17.8-2.6, G54.4-0.3, G127.1+0.5, G132.7+1.3, G332.0+0.2

1. MODELS OF SHELL SUPERNOVA REMNANTS EMISSION

Supernova remnants (SNRs) are among the strongest synchrotron sources in the Milky Way and other galaxies. We consider two models of shell SNRs emission: an optically thin shell with constant emissivity and an optically thin synchrotron shell with radially aligned magnetic field. Here, only final results are given. For theoretical details, see Arbutina and Opsenica (2012). A hypothetical shell SNR is shown in Fig. 1.

1.1. Model with constant emissivity

The constant emissivity model intensity of emitted radiation is given by formula:

$$I_\nu = \begin{cases} C_\nu \left(\sqrt{\sin^2 \theta_2 - \sin^2 \theta} - \sqrt{\sin^2 \theta_1 - \sin^2 \theta} \right), & 0 < \theta < \theta_1 \\ C_\nu \sqrt{\sin^2 \theta_2 - \sin^2 \theta}, & \theta_1 \leq \theta \leq \theta_2, \end{cases} \quad (1)$$

where $\theta_1 = \arcsin \frac{R-\Delta}{d}$, $\theta_2 = \arcsin \frac{R}{d}$ and $C_\nu = 2\varepsilon_\nu d$.

The emissivity, which is constant in this model, is denoted by ε_ν , where ν is the observed frequency. Radius is denoted by R , Δ is shell thickness and d distance to the remnant. The graphical representation of Eq. (1) is shown in Fig. 2. The flux density is given by the formula:

$$S_\nu = \frac{2\pi}{3} C_\nu (\sin^3 \theta_2 - \sin^3 \theta_1). \quad (2)$$

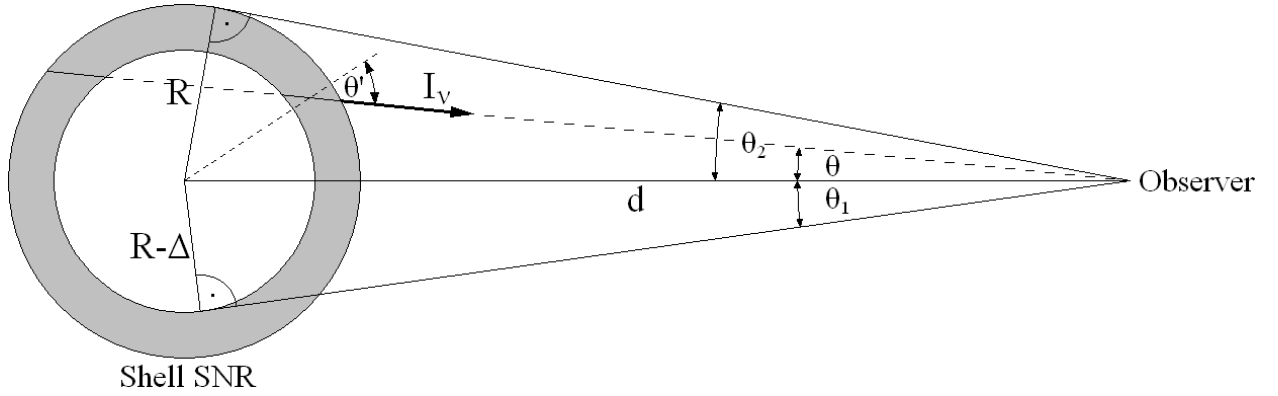


Fig. 1. Linear and angular dimensions of a shell SNR model.

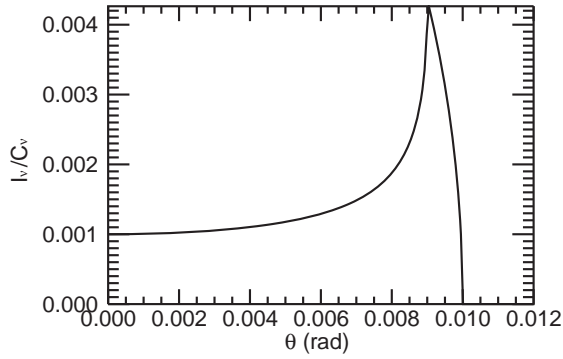


Fig. 2. Graphical representation of Eq. (1), assuming $\theta_1 = 0.009$ rad and $\theta_2 = 0.01$ rad.

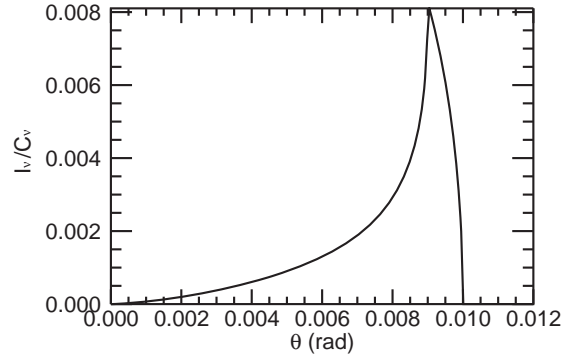


Fig. 3. Graphical representation of Eq. (3), assuming $\theta_1 = 0.009$ rad, $\theta_2 = 0.01$ rad and $\alpha = 0.5$.

1.2. Model with radial magnetic field

In the case of this model, intensity of synchrotron radiation is given by:

$$I_\nu = \begin{cases} 2C_\nu \sin \theta \int_{\mu_{1-}}^{\mu_{2-}} (1 - \mu^2)^{\frac{\alpha-2}{2}} d\mu, & 0 < \theta < \theta_1 \\ C_\nu \sin \theta \int_{\mu_{2+}}^{\mu_{1+}} (1 - \mu^2)^{\frac{\alpha-2}{2}} d\mu, & \theta_1 \leq \theta \leq \theta_2, \end{cases} \quad (3)$$

where $\mu = \cos \theta'$, $\mu_{1,2\pm} = \mp \frac{\sqrt{\sin^2 \theta_{1,2} - \sin^2 \theta}}{\sin \theta_{1,2}}$, $\theta_1 = \arcsin \frac{R-\Delta}{d}$, $\theta_2 = \arcsin \frac{R}{d}$ and $C_\nu = \tilde{\epsilon}_\nu d$.

Emissivity is given by $\epsilon_\nu = \tilde{\epsilon}_\nu (\sin \theta')^{\alpha+1}$, where $\tilde{\epsilon}_\nu \propto B^{\alpha+1} \nu^{-\alpha}$. Magnetic field is denoted by B and α is spectral index which has average value of 0.5 for SNRs. The angle between line of force of the magnetic field and line of sight is θ' . Graphical representation of Eq. (3) is shown in Fig. 3. The flux density is given by:

$$S_\nu = \frac{2\pi\sqrt{\pi}}{3} \frac{\Gamma(\frac{\alpha+3}{2})}{\Gamma(\frac{\alpha+4}{2})} C_\nu (\sin^3 \theta_2 - \sin^3 \theta_1). \quad (4)$$

2. INTERACTIVE DATA LANGUAGE (IDL) CODES

2.1. Direct problem: simulation of observations of shell SNRs with radio telescope

When we observe an object in the sky with a radio telescope, image that we obtain is a convolution of real intensity of emission of the object and power pattern of the telescope:

$$I_\nu^{\text{conv}}(\theta_0, \varphi_0) = \frac{\int_0^\pi \int_0^{2\pi} I_\nu(\theta, \varphi) P_n(\theta'') \sin \theta d\theta d\varphi}{\int_0^\pi \int_0^{2\pi} P_n(\theta) \sin \theta d\theta d\varphi}, \quad (5)$$

where $I_\nu(\theta, \varphi)$ is the real intensity of and $P_n(\theta)$ is the power pattern of the radio telescope. Angle θ'' is related to other angular parameters through following relation of spherical trigonometry:

$$\cos \theta'' = \cos \theta \cos \theta_0 + \sin \theta \sin \theta_0 \cos (\varphi - \varphi_0), \quad (6)$$

as it can be seen from Fig. 4. Here, we assumed that power pattern is symmetrical, so it does not depend on variable φ .

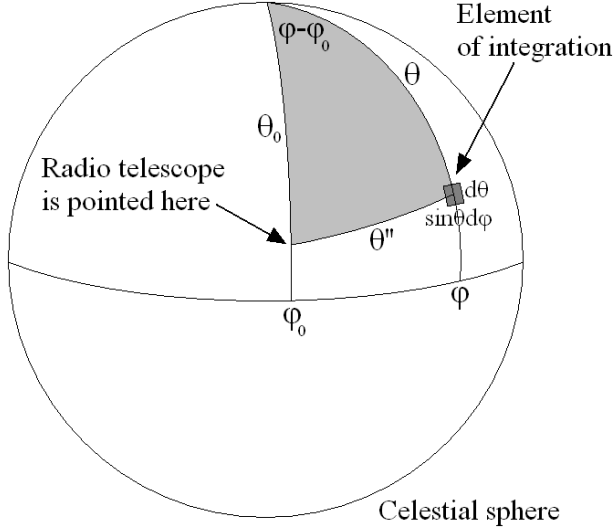


Fig. 4. Schematic representation of angles from Eq. (6) on celestial sphere. Element of double integration of Eq. (5) is also shown.

If convolution (5) is simulated numerically, it must be assumed that power pattern takes zero value for angles greater than some critical angle θ_c , because of technical limitations. For power pattern $P_n(\theta)$, two possible cases have been chosen: Gaussian approximation and approximation with Bessel function of the first kind.

- (i) In the case of Gaussian approximation, the power pattern is given by:

$$P_n(\theta) = \begin{cases} e^{-a\theta^2}, & \theta \leq \theta_c \\ 0, & \theta > \theta_c, \end{cases} \quad (7)$$

where $a = \frac{4 \ln 2}{\text{HPBW}^2}$. HPBW stands for Half Power Beam Width. In the case of Gaussian approximation of power pattern, θ_c of 5σ is used, where σ is an angle at which Gaussian power pattern takes value $\frac{1}{e}$, and it is equal to $\frac{1}{\sqrt{a}}$.

- (ii) In the case of approximation with Bessel function of the first kind, the power pattern is given by:

$$P_n(\theta) = \begin{cases} \left[\frac{2J_1\left(\frac{\pi D}{\lambda} \sin \theta\right)}{\frac{\pi D}{\lambda} \sin \theta} \right]^2, & \theta \leq \theta_c, \\ 0, & \theta > \theta_c, \end{cases} \quad (8)$$

where $J_1(x)$ is Bessel function of the first kind, D is the diameter of radio telescope, and λ is the wavelength of observed emission from an SNR. For Bessel

function approximation $\text{HPBW} = 1.02 \frac{\lambda}{D}$ (Urošević and Milogradov-Turin 2007, Wilson et al. 2009). In this case θ_c equal to 8 HPBW is used.

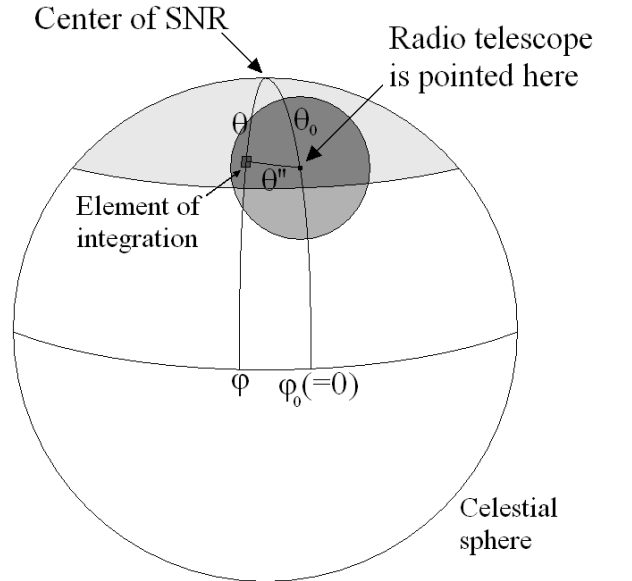
Expression that is used for numerical simulation of convolution of radiation intensity and power pattern of a radio telescope is:

$$I_\nu^{\text{conv}}(\theta_0) = \frac{\int \int_{\text{Intersection}} I_\nu(\theta) P_n(\theta'') \sin \theta d\theta d\varphi}{2\pi \int_0^{\theta_c} P_n(\theta) \sin \theta d\theta}. \quad (9)$$

Here $I_\nu(\theta)$ is one of the expressions (1) or (3), according to chosen model of SNR emission, and $P_n(\theta)$ is one of the expressions (7) and (8), according to chosen power pattern approximation. Angle θ'' is related to other angular parameters through following relation of spherical trigonometry:

$$\cos \theta'' = \cos \theta \cos \theta_0 + \sin \theta \sin \theta_0 \cos \varphi, \quad (10)$$

as it can be seen from Fig. 5. Convolved intensity does not depend on φ_0 , so we took $\varphi_0 = 0$ (see Eq. 9).



- Region of SNR model (angular radius of this region is θ_2)
- Region where power pattern of radio telescope has value greater than zero (angular radius of this region is θ_c)
- Intersection between the two regions

Fig. 5. Schematic representation of angles from Eq. (10) on celestial sphere. Element of double integration from numerator of Eq. (9) is also shown.

Region of double integration in the numerator of Eq. (9) is the intersection between regions of SNR model and power pattern (the intersection is shown in Fig. 5). This double integration is performed by the IDL function `INT_2D`. Integration in denominator of Eq. (9) is performed by the IDL function `QROMB`.

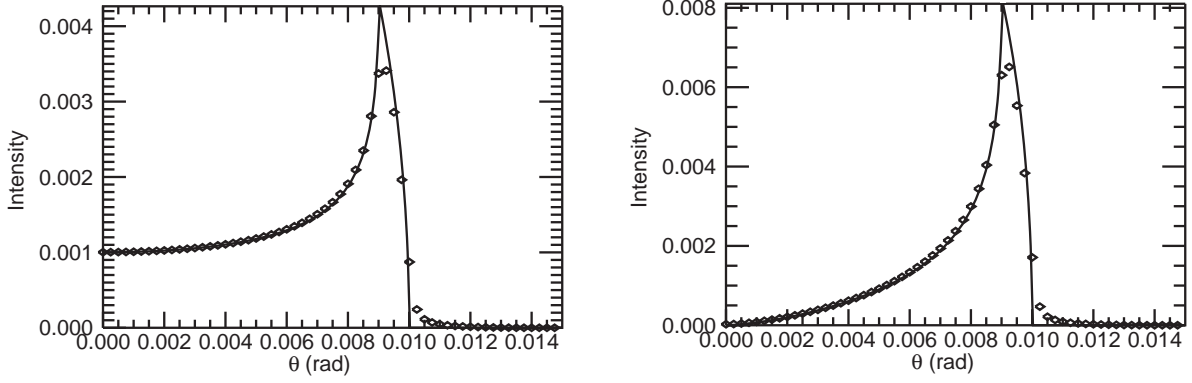


Fig. 6. Simulated convolutions for the two considered models. The real intensity of SNR's emission is shown by a full line, convolved intensity by diamonds. Angular dimensions in radians are given on abscissas, intensity of emission on ordinates. Left: model with constant emissivity ($\theta_1 = 0.009$ rad, $\theta_2 = 0.01$ rad); right: model with radial magnetic field ($\theta_1 = 0.009$ rad, $\theta_2 = 0.01$ rad, $\alpha = 0.5$). Approximation of power pattern with Bessel function of the first kind with $HPBW = 5 \cdot 10^{-4}$ rad was used.

Integrations in Eq. (3) are performed by the IDL functions `QROMB` and `INT_TABULATED`, as well as by a "handwritten" function that calculates definite integrals using rectangular method.

For the first model (with constant emissivity), user of the program enters parameters C_ν , θ_1 , θ_2 , as well as parameter of antenna $HPBW$, and the program performs a convolution. For the second model (with radial magnetic field), user also enters an additional parameter - spectral index α . The simulated convolutions for two considered models are shown in Fig. 6.

2.2. Indirect problem: fitting observed profile of SNR

User provides observed radial emission profile of a shell SNR in the form of a table, as well as the parameter $HPBW$. By fitting the data to a chosen model, the program finds the best values for parameters C_ν , θ_1 and θ_2 in the case of the first model, or C_ν , θ_1 , θ_2 and α , in the case of the second model. This is performed by the iterative IDL procedure `CURVEFIT`. To perform this procedure, user has to estimate the initial values for the parameters. The initial values for the parameters θ_1 and θ_2 , as well as value of $I_\nu(\theta_1)$, can be estimated from observational data when the mean profile of observed SNR is calculated (see Fig. 7). The initial value for spectral index $\alpha = 0.5$ can be used. The initial value for C_ν can be estimated from the following equations:

$$C_\nu^{\text{init}} = \frac{I_\nu(\theta_1^{\text{init}})}{\sqrt{\sin^2 \theta_2^{\text{init}} - \sin^2 \theta_1^{\text{init}}}}, \quad (11)$$

for the model with constant emissivity, and

$$C_\nu^{\text{init}} = \frac{I_\nu(\theta_1^{\text{init}})}{2 \sin \theta_1^{\text{init}} \int_0^{\mu_c} (1 - \mu^2)^{\frac{\alpha^{\text{init}} - 2}{2}} d\mu}, \quad (12)$$

where $\mu_c = \sqrt{1 - \left(\frac{\sin \theta_1^{\text{init}}}{\sin \theta_2^{\text{init}}}\right)^2}$, for the model with radial magnetic field. The integral from Eq. (12) can be calculated using the IDL function `QSIMP` or `QROMB`.

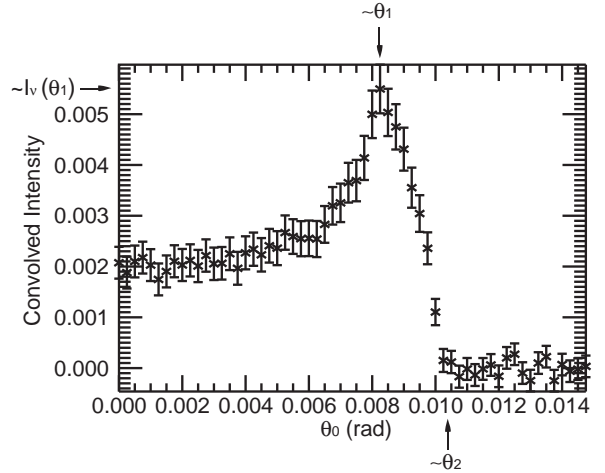


Fig. 7. Scheme for estimating initial values of the parameters θ_1 and θ_2 , and value of $I_\nu(\theta_1)$. The data points and the error bars are artificially generated.

In addition to finding the best values of parameters, the program also calculates their errors (i.e. standard deviations). Finally, the program calculates the integrated flux density of an SNR using Eqs. (2) or (4), and its error, using equations:

$$\frac{\Delta S_\nu}{S_\nu} = \frac{\Delta C_\nu}{C_\nu} + 3 \frac{\sin^2 \theta_2 \cos \theta_2 \Delta \theta_2 + \sin^2 \theta_1 \cos \theta_1 \Delta \theta_1}{\sin^3 \theta_2 - \sin^3 \theta_1}, \quad (13)$$

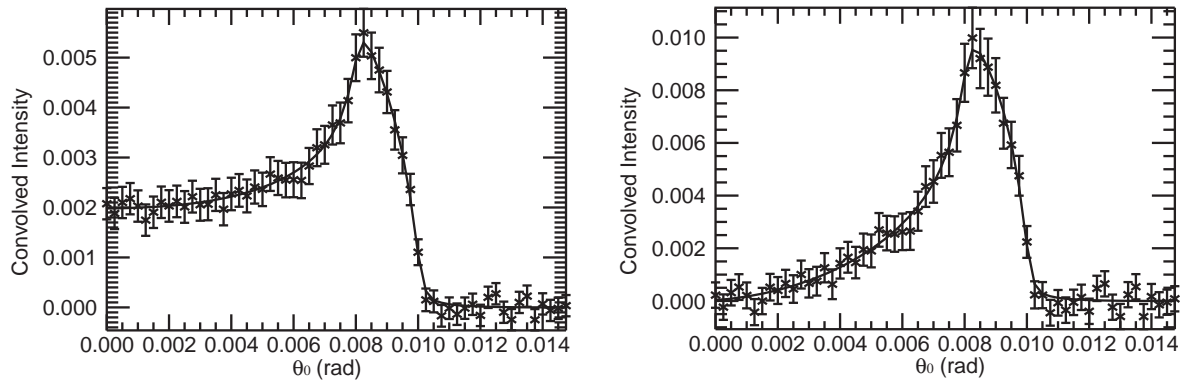


Fig. 8. Examples of fitted radial emission profiles of SNRs for the two considered models. Artificially generated mean radial emission profiles of SNRs are shown by "X" symbols with error bars, fitted (best) profiles as full lines. Angular dimensions in radians are given on abscissas, intensity of emission on ordinates. Left: model with constant emissivity; right: model with radial magnetic field.

in the case of model with constant emissivity, and

$$\frac{\Delta S_\nu}{S_\nu} = \frac{\Delta C_\nu}{C_\nu} + 3 \frac{\sin^2 \theta_2 \cos \theta_2 \Delta \theta_2 + \sin^2 \theta_1 \cos \theta_1 \Delta \theta_1}{\sin^3 \theta_2 - \sin^3 \theta_1} + \frac{1}{2\Gamma(\frac{\alpha+3}{2})} \frac{d\Gamma(t)}{dt} \Big|_{t=\frac{\alpha+3}{2}} \Delta\alpha + \frac{1}{2\Gamma(\frac{\alpha+4}{2})} \frac{d\Gamma(t)}{dt} \Big|_{t=\frac{\alpha+4}{2}} \Delta\alpha, \quad (14)$$

in the case of a model with radial magnetic field where ΔC_ν , $\Delta \theta_1$, $\Delta \theta_2$ and $\Delta \alpha$ are the errors of the parameters C_ν , θ_1 , θ_2 and α respectively. Gamma function could be calculated using the IDL function `GAMMA`. Derivative of gamma function could be calculated using the expression: $\frac{d\Gamma(t)}{dt} = \int_0^\infty x^{t-1} e^{-x} \ln x dx$. The integral from the last expression can be calculated using the IDL function `QROMO`. Examples of fitted radial profiles of SNRs for the two considered models are shown on Fig. 8.

This method of determining parameters and flux densities of SNRs from radio observations has some disadvantages. Potential user of this numerical method should have several facts in mind:

- Generally, real shell SNRs are not completely spherical;
- This method uses approximative power pattern of a radio telescope;
- The magnetic field is not radially aligned (this refers to the second model);
- The sensitivity of the second model to parameter α is very weak, so this method can not determine it successfully enough. It is recommended that one uses value of α that is deter-

mined from spectrum of SNR if available. In that case, the parameter α should be fixed in the iterative procedure of determining parameters.

- Final values of parameters somewhat depend on initial values, which is the case with all non-linear fitting methods.

3. APPLICATION OF THE IDL CODES TO OBSERVED SNR PROFILES

We applied our numerical method to several shell SNRs observed with Effelsberg radio telescope in Germany (Reich et al. 1984, Reich et al. 1990, Fuerst et al. 1990) and from the MOST supernova remnant catalogue (MSC). Observations given in MSC were made with Molonglo Observatory Synthesis Telescope (MOST) in Australia that operates at 843 MHz (Whiteoak and Green 1996).

Firstly, FITS (Flexible Image Transport System) images of SNRs have been downloaded from web-sites of the above databases (Effelsberg and MOST).¹ Secondly, mean radial emission profiles were extracted from the FITS files using programs "SAOImage DS9" and "Funtools".² With "Funtools", it is possible to exclude unwanted regions from a FITS image and to subtract a background prior to calculating the mean radial emission profile.

¹<http://www.mpifr-bonn.mpg.de/survey.html>, <http://www.physics.usyd.edu.au/sifa/Main/MSC>

²<http://hea-www.harvard.edu/RD/ds9/>, <http://hea-www.harvard.edu/saord/funtools/>

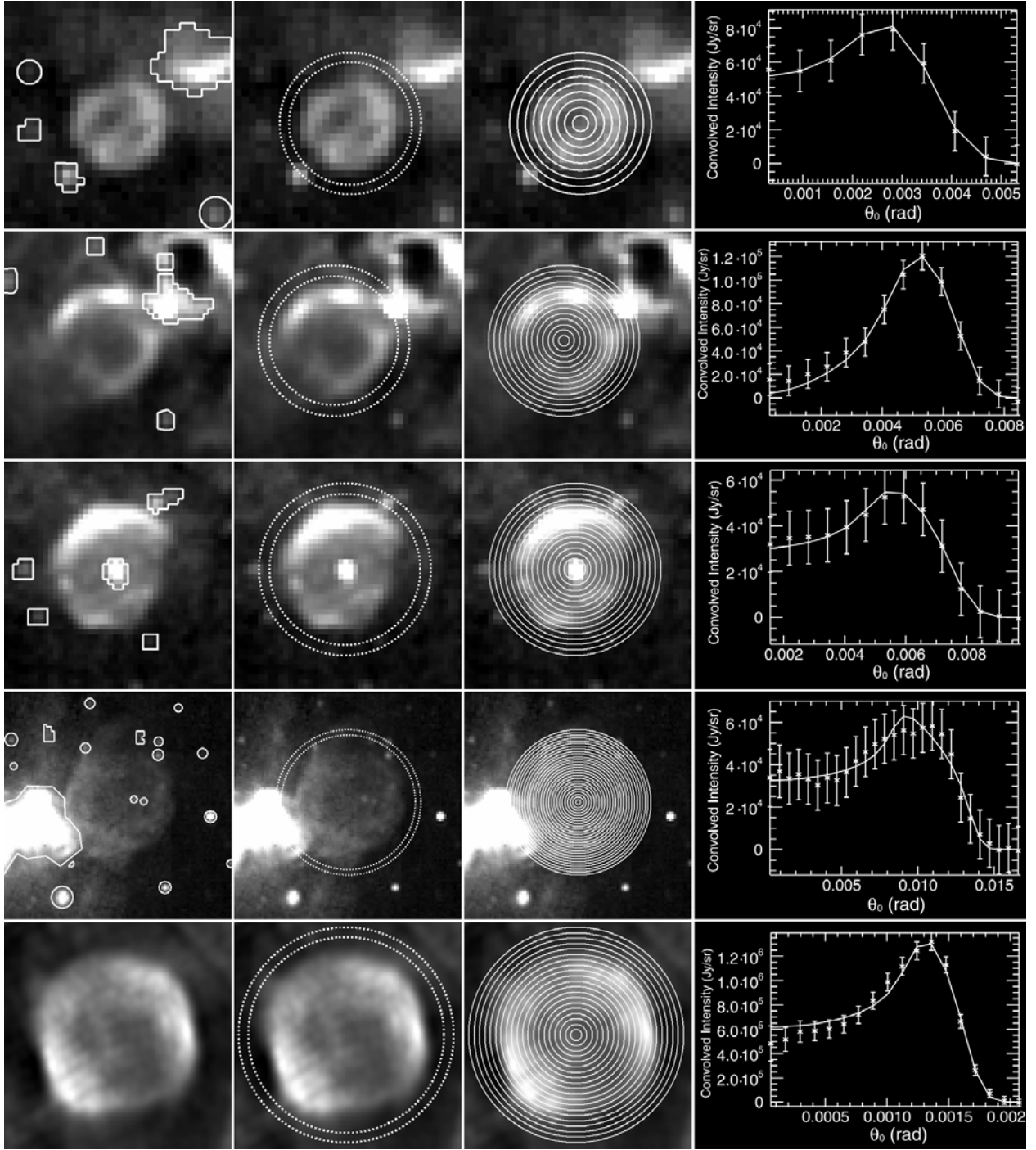


Fig. 9. Five shell SNRs whose mean radial emission profiles were fitted well. From left to right: excluded regions, background region, annuli regions, fitted mean radial emission profile. From up to down: SNR G17.8-2.6, SNR G54.4-0.3, SNR G127.1+0.5, SNR G132.7+1.3, SNR G332.0+0.2. Graphs: angular dimensions in radians are given on abscissas, intensity of emission in Jy/sr on ordinates. Observed (mean) profiles are depicted by "X" symbols with error bars, while fitted theoretical profiles are plotted as solid lines. Mean radial emission profile of the SNR G54.4-0.3 is fitted by the model with radial magnetic field, while profiles of the other SNRs are fitted by the model with constant emissivity. Out of these five SNRs, only SNR G332.0+0.2 is from the MOST catalogue, while the others are from the Effelsberg survey.

In order to obtain the mean radial emission profile, we first exclude unwanted regions, i.e. regions that do not belong to an SNR, but are close or within its boundaries. We achieve this by using polygonal and circular shapes in DS9. We determine a background by an annulus region in DS9. The background region should be just beyond the outer boundary of an SNR. Then, we make annular regions in DS9 that consist of concentric rings and are centered at approximate SNR center (in our case, an angular distance between adjacent rings was chosen to be HPBW/2). Finally, Funtools averages pixel value over those annular regions and subtract average value of a pixel within a background region from each counted annular value (both of that without taking excluded regions into account) and a mean radial emission profile is calculated. Data point units of that profile are the same as tabular units in the corresponding FITS file.

Tabular units in Effelsberg FITS files were mK (miliKelvin). Conversion to units Jy/sr (Jansky/steradian) was made by multiplying tabular values by the factor $10^{-3} \times 10^{26} \times \frac{2k\nu^2}{c^2} = 10^{23} \times \frac{2k\nu^2}{c^2}$, where $k = 1.38 \times 10^{-23} \frac{\text{J}}{\text{K}}$, $\nu = 2.695 \times 10^9 \text{ Hz}$ and $c = 3 \times 10^8 \frac{\text{km}}{\text{s}}$. The tabular units in FITS files from the MOST SNR catalogue were Jy/beam. Conversion to units Jy/sr was made using the formula (Kameno 2007):

$$\left(\frac{I_\nu}{\text{Jy/sr}}\right) = 3.75479 \times 10^{10} \times \left(\frac{\text{HPBW}_{\text{maj}}}{\text{arcsec}}\right)^{-1} \times \left(\frac{\text{HPBW}_{\text{min}}}{\text{arcsec}}\right)^{-1} \times \left(\frac{S}{\text{Jy/beam}}\right), \quad (15)$$

where HPBW_{maj} and HPBW_{min} are HPBWs along major and minor axes (MOST is a synthesis telescope that has asymmetrical power pattern). To convert Kelvins to Jy/beam one can use formula (Kameno 2007):

$$\left(\frac{T_{\text{B}}}{\text{K}}\right) = 1.222 \times 10^6 \times \left(\frac{\text{HPBW}_{\text{maj}}}{\text{arcsec}}\right)^{-1} \times \left(\frac{\text{HPBW}_{\text{min}}}{\text{arcsec}}\right)^{-1} \times \left(\frac{\nu}{\text{GHz}}\right)^{-2} \times \left(\frac{S}{\text{Jy/beam}}\right). \quad (16)$$

Sensitivity of the Effelsberg observations is 50 mK (20 mJy/beam), while sensitivity of the MOST telescope is 2 mJy/beam. Errors of mean profile data points were calculated as sum of errors that are derived from these sensitivities, and errors that are calculated by the program "Funtools" during the process of extracting mean profiles:

$$\Delta I_\nu^{\text{Mean profile}} = \Delta I_\nu^{\text{Sensitivity}} + \Delta I_\nu^{\text{Funtools}}. \quad (17)$$

The appropriate model was chosen and fitted to each of the extracted mean radial emission profiles. Power pattern approximation used in the process of fitting was Gaussian. Effelsberg HPBW was 4.3 arcmin. For the MOST, HPBW is not constant along different axes but is given by $\text{HPBW} = 43 \text{ arcsec} \times 43 \text{ arcsec} \cdot \cos \delta$ where δ is a declination of observed point on celestial sphere. Because of that, we used "effective" HPBW that is equal to $\sqrt{\text{HPBW}_{\text{maj}} \cdot \text{HPBW}_{\text{min}}}$, or:

$$\text{HPBW}_{\text{eff}} = \sqrt{43 \text{ arcsec} \times 43 \text{ arcsec} \cdot \cos \delta}, \quad (18)$$

while δ was taken to be a declination of center of the considered SNR.

4. RESULTS AND CONCLUSIONS

To test the code with real SNRs, we searched the two databases mentioned above for all SNRs marked as spherical (with only one value for radius listed). Out of ten SNRs whose mean radial emission profiles were fitted, profiles of five were fitted well. Other five are either weak radio-continuum emitters (G180.0-1.7, G294.1-0.0, G299.6-0.5, G321.9-1.1), or our models seem to be inadequate (G359.1-0.5). The five well fitted SNRs and their mean radial emission profiles are shown in Fig. 9. Parameters which are obtained from the fit are shown in Table 1. We also estimated flux densities of these SNRs at the frequency of 1 GHz using formula:

Table 1. Parameters of five shell SNRs whose mean radial emission profiles were fitted well.

SNR	α (from Green's catalogue)	ν [GHz] (observed frequency)	$C_\nu \left[\frac{\text{Jy}}{\text{sr}}\right]$ (from fit)	θ_1 [rad] (from fit)	θ_2 [rad] (from fit)
G17.8-2.6	0.3?	2.695	$(3.5 \pm 0.7) \cdot 10^7$	$(2.5 \pm 0.3) \cdot 10^{-3}$	$(4.0 \pm 0.2) \cdot 10^{-3}$
G54.4-0.3	0.5	2.695	$(1.7 \pm 0.3) \cdot 10^7$	$(4.7 \pm 0.3) \cdot 10^{-3}$	$(6.8 \pm 0.2) \cdot 10^{-3}$
G127.1+0.5	0.45	2.695	$(1.1 \pm 0.4) \cdot 10^7$	$(5.2 \pm 0.6) \cdot 10^{-3}$	$(7.9 \pm 0.5) \cdot 10^{-3}$
G132.7+1.3	0.6	2.695	$(6.4 \pm 0.9) \cdot 10^6$	$(8.7 \pm 0.6) \cdot 10^{-3}$	$(1.38 \pm 0.05) \cdot 10^{-2}$
G332.0+0.2	0.5	0.843	$(1.4 \pm 0.1) \cdot 10^9$	$(1.25 \pm 0.03) \cdot 10^{-3}$	$(1.70 \pm 0.02) \cdot 10^{-3}$

Table 2. Parameters θ_1 and θ_2 in arcminutes and flux densities of analysed SNRs.

SNR	θ_1 [arcmin] (from fit)	θ_2 [arcmin] (from fit)	S_ν [Jy] (calculated)	S_ν [Jy] (observed)	$S_{1\text{ GHz}}$ [Jy] (calculated)	$S_{1\text{ GHz}}$ [Jy] (from Green's catalogue)
G17.8-2.6	8.8 ± 0.8	13.6 ± 0.6	3 ± 2	3.4 ± 0.9	$5 \pm 3 ?$	4.0?
G54.4-0.3	16.2 ± 0.8	23.5 ± 0.7	11 ± 4	11 ± 2	18 ± 7	28
G127.1+0.5	18 ± 2	27 ± 2	8 ± 5	8 ± 3	12 ± 8	12
G132.7+1.3	30 ± 2	47 ± 2	26 ± 9	26 ± 9	50 ± 20	45
G332.0+0.2	4.29 ± 0.09	5.85 ± 0.06	8 ± 2	8.5 ± 0.5	7.8 ± 1.2	8?

$$S_{1\text{ GHz}} = S_\nu \left(\frac{\nu}{1\text{ GHz}} \right)^\alpha, \quad (19)$$

where S_ν is the flux density at frequency ν and α is spectral index. Note that these flux densities S_ν and $S_{1\text{ GHz}}$ (labeled as "calculated" in Table 2) do not represent real flux densities directly obtained from observations. They are calculated from the fit, using Eqs. (2), (4) and (19).

The real flux densities at the observed frequency ν (labeled as "observed" in Table 2) are also determined, this time by summing pixel values over inner circles of the background regions, multiplied by solid angle of one pixel. In the case of SNRs G127.1+0.5 and G132.7+1.3 where excluded regions exist within an SNR, we filled these "gaps" with average values of a pixel around borders of these excluded regions. Background subtraction, conversion of units and error calculation were performed in the same manner as in the case of calculating mean profiles. Spectral indices α and values of flux densities $S_{1\text{ GHz}}$ that we compared our calculated values to, are taken from "A Catalogue of Galactic Supernova Remnants" (Green 2009).³

We conclude that good results are obtained in five of ten considered cases, which justify the use of our code for remnants that are bright (so that observational errors are not large) and spherically symmetric enough. Application of our code to a larger sample of SNRs is planned for future work.

Acknowledgements – During the work on this paper the authors were financially supported by the Ministry of Education and Science of the Republic of

Serbia through the projects: 176004 'Stellar physics' and 176005 'Emission nebulae: structure and evolution'.

The MOST is operated by The University of Sydney with support from the Australian Research Council and the Science Foundation for Physics within The University of Sydney.

This research has made use of NASA's Astrophysics Data System (ADS) and SAOImage DS9, developed by Smithsonian Astrophysical Observatory.

REFERENCES

- Arbutina, B. and Opsenica, S.: 2012, *Publ. Astron. Obs. Belgrade*, in press.
- Fürst, E., Reich, W., Reich, P. and Reif, K.: 1990, *Astron. Astrophys. Suppl. Series*, **85**, 691.
- Green, D. A.: 2009, *Bull. Astr. Soc. India*, **37**, 45.
- Kameno, S.: 2007, Map to Science, Asian Radio Astronomy Winter School 2007.
- Reich, W., Fürst, E., Reich, P. and Reif, K.: 1990, *Astron. Astrophys. Suppl. Series*, **85**, 633.
- Reich, W., Fürst, E., Steffen, P., Reif, K. and Haslam, C. G. T.: 1984, *Astron. Astrophys. Suppl. Series*, **58**, 197.
- Urošević, D. and Milogradov-Turin, J.: 2007, Teorijske osnove radio-astronomije, Matematički fakultet, Beograd.
- Whiteoak, J. B. Z. and Green, A. J.: 1996, *Astron. Astrophys.*, **118**, 329.
- Wilson, T. L., Rohlfs, K. and Hüttemeister, S.: 2009, Tools of Radio Astronomy, Springer-Verlag Berlin Heidelberg.

³<http://www.mrao.cam.ac.uk/surveys/snrs/>

**НУМЕРИЧКИ КОД ЗА ФИТОВАЊЕ РАДИЈАЛНОГ ЕМИСИОНОГ
ПРОФИЛА ЉУСКАСТОГ ОСТАТКА СУПЕРНОВЕ. ПРИМЕНА**

S. Opsenica and B. Arbutina

*Department of Astronomy, Faculty of Mathematics, University of Belgrade
Studentski trg 16, 11000 Belgrade, Serbia*

E-mail: *slobodan@math.rs, arbo@math.rs*

УДК 524.354–17–77

Претходно саопштење

Написани су IDL кодови који служе за фитовање средњег профила љускастог остатка супернове добијеног радио-посматрањима једним од два теоријска модела емисије. Моделли који су разматрани су: 1) љуска са константном емисивношћу и 2) љускасти извор синхротронског зрачења са радијално оријентисаним магнетним пољем. Кодови су при-

мењени на неколико посматраних остатака супернових. У пет разматраних случајева добијени су добри резултати, што оправдава коришћење датог кода за остатке који су довољно сјајни (тако да посматрачке грешке нису велике) и у довољној мери сферносиметрични.